Inorg. Chem. **2008**, *47*, 6173−6183

Anion Detection by Fluorescent Zn(II) Complexes of Functionalized Polyamine Ligands

Laura Rodríguez,[†] João C. Lima,[†] A. Jorge Parola,[†] Fernando Pina,*[,†] Robert Meitz,[‡] Ricardo Aucejo,[‡] Enrique Garcia-España,*[,‡] José M. Llinares,[§] Conxa Soriano,[§] and Javier Alarcón[||]

Departamento de Química, REQUIMTE, Faculdade de Ciências e Tecnologia, Universidade Nova de Lisboa, Portugal, Instituto de Ciencia Molecular (ICMOL), Departament de Química Inorgànica, Facultat de Química, Universitat de València, Paterna, Spain, Instituto de Ciencia Molecular (ICMOL), Departament de Química Orgànica, Facultat de Farmàcia, Universitat de València, Burjassot, Spain, and Departament de Química Inorgànica, Facultat de Química, Universitat de València, Burjassot, Spain

Received December 11, 2007

The Zn^{2+} coordination chemistry and luminescent behavior of two ligands constituted by an open 1,4,7-triazaheptane chain functionalized at both ends with 2-picolyl units and either a methylnaphthyl (**L1**) or a dansyl (**L2**) fluorescent unit attached to the central amino nitrogen are reported. The fluorescent properties of the Zn**L1**$^{2+}$ and Zn**L2**$^{2+}$ complexes are then exploited toward detection of anions. **L1** in the pH range of study has four protonation constants. The fluorescence emission from the naphthalene fluorophore is quenched either at low or at high pH values leading to an emissive pH window centered around pH = 5. In contrast, in **L2** the fluorescence emission from the dansyl unit occurs only at basic pH values. In the case of **L1**, a red-shifted band appearing in the visible region was assigned to an exciplex emission involving the naphthalene and the tertiary amine of the polyamine chain. **L1** forms Zn^{2+} mononuclear complexes of ZnH_p**L1**$^{(p+2)+}$ stoichiometry with $p = 1, 0, -1$. Formation of the Zn**L1**$^{2+}$species produces a strong enhancement of the **L1** luminescence leading to an extended emissive pH window from pH = 5 to pH = 9. Addition of several anions to this last complex leads to a partial quenching effect. On the contrary, the fluorescence emission of **L2** is partially quenched upon complexation with Zn^{2+} in the same pH window ($5 < pH < 9$). The lower stability of Zn**L2**$^{2+}$ with respect to Zn**L1**$^{2+}$ suggests a lack of involvement of the sulfonamide group in the first coordination sphere. However, there is spectral evidence for an interesting photoinduced binding of the sulfonamide nitrogen to Zn^{2+}. While addition of diphosphate, triphospate, citrate, and D,L-isocitrate to a solution of Zn**L2**$^{2+}$ restores the fluorescence emission of the system (λ_{max} ca. 600 nm), addition of phosphate, chloride, iodide, and cyanurate do not produce any significant change in fluorescence. Moreover, this system would permit one to differentiate diphosphate and triphosphate over citrate and D,L-isocitrate because the fluorescence enhancement observed upon addition of the first anions is much sharper. The Zn**L2**$^{2+}$ complex and its mixed complexes with diphosphate, triphosphate, citrate, and D,L-isocitrate have been characterized by ^{1}H, ^{31}P NMR, and Electrospray Mass Spectrometry.

Introduction

In spite of the great efforts devoted to the design of organic receptors for the efficient and selective binding of anions carried out since the 1970s, the number of chemosensors for anions is still limited when compared with the numerous sensors for cations described in the literature.[1] Because anions play a crucial role in chemistry and biology, this topic is of great interest. In particular fluorescent chemosensors for anions are very appealing because this technique usually exhibits low detection limits, and a spectrofluorimeter is equipment available in many laboratories.[2]

In recent years a great deal of experimental work has been devoted to molecular fluorescent chemosensors bearing polyamine chains as receptor units.[3] The polyamine chains are extremely useful for anion binding because they can be protonated at relatively high pH values, where many anions

* To whom correspondence should be addressed. E-mail: fjp@dq.fct.unl.pt (F.P.), enrique.garcia-es@uv.es (E.G.-E.). Phone: +351 212948355(F.P.), +34 963544879(E.G.-E.). Fax: +351 212948550 (F.P.), +34 963864322 (E.G.-E.).

[†] REQUIMTE, Universidade Nova de Lisboa.

[‡] Instituto de Ciencia Molecular (ICMOL), Departament de Química Inorgànica, Facultat de Química, Universitat de València.

[§] Facultat de Farmàcia, Universitat de València.

[||] Departament de Química Inorgànica, Facultat de Química, Universitat de València.

10.1021/ic7023956 CCC: $40.75 © 2008 American Chemical Society
Published on Web 06/26/2008

are still negatively charged. This favorable situation permits the use of electrostatic interactions and in some cases hydrogen bonding as a driving force to bind anions. One drawback of polyamines is the absence of intrinsic fluorescence, which is overcome by appending fluorescent units, in most cases aromatic hydrocarbons such as anthracene or naphthalene. This procedure matches the concept of a combined chemosensor: a binding unit and a signaling unit linked by a spacer.[4,5] In general, polyamines quench the emission of the aromatic signaling unit by photoinduced electron transfer (PET). However, protonation of the amines or coordination to full d shell metal ions, as for example Zn^{2+} and Cd^{2+}, prevents the quenching mechanism and allows the emission of the signaling unit to appear.[5,6] In some receptor units, aromatic nitrogen heterocycles like pyridine have been integrated in the ligand to modulate its binding properties. In these cases, protonation of the aromatic nitrogen at acidic pH values also gives rise to PET from the excited fluorophore to the protonated heterocycle, resulting in fluorescence quenching.[6] Systems containing both aliphatic amines and nitrogen heterocycles are only effective in a pH window whose width is dependent on the structure of the molecule.

Sensing of anions by means of chemosensors based on polyamine receptors can occur by direct binding of the anion to the receptor unit as it has been shown to occur, for instance, for the nucleotide 5′-adenosine triphosphate (ATP).[7] Alternatively, anions can be sensed by interaction through coordinative bond formation with strongly emissive binary metal complexes like those of Zn^{2+}. To achieve such a situation, the coordination sphere of the metal ion has either not to be fully saturated by the donor atoms of the ligands or it should have ligands readily removable by the donor atoms of the incoming anion. Although this alternative has not been as widely explored as the previous one, it offers interesting possibilities in terms of selectivity and sensitivity because of the intrinsic characteristics of the coordinative bond. The recent work of Hamachi et al. on the development of Zn(II) complexes as fluorescent sensors for phosphorylated species constitutes a good example of this strategy.[8]

With this purpose, we report two examples of ternary Zn^{2+}-**L**-Anion systems, both bearing two 2-pycolyl groups, the first one (**L** = **L1**) sensing anions by Chelation Enhancement of the Quenching (CHEQ) and the second one (**L** = **L2**) by Chelation Enhancement of the Fluorescence (CHEF), see Scheme 1. In the case of the Zn^{2+}-**L2** system, which presents the best discrimination behavior for anionic species, the binary and ternary complexes have been additionally identified by ^{1}H and ^{31}P NMR apart from electrospray mass spectrometry (ESI).

Results and Discussion

Free Ligands. Naphthalene Sensing Unit. The pH-dependent absorption spectra of compound **L1** (Figure 1A) shows the superimposed contributions from the two chromophores (pyridine and naphthalene). The pyridine absorption occurs at around 260 nm and its intensity increases upon protonation, whereas the naphthalene contribution is pH independent with a maximum at approximately 275 nm. This is in agreement with identical observations previously reported for compound **L3**.[9]

The pH dependence of the fluorescence emission spectra of compound **L1** is shown in Figure 1B. The spectra are dominated by the emission of the naphthalene centered at 335 nm, presenting also an additional structureless band at lower energies (λ_{max} = 440 nm), assignable to an exciplex emission due to a charge transfer from the tertiary amine lone pair to the excited naphthalene.[10]

The ratio of the exciplex to naphthalene bands (ϕ_{Exc}/ϕ_{N}) can be described by eq 1, within the framework of the kinetic

(1) (a) *Supramolecular Chemistry of Anions*; Bianchi, A., Bowman-James, K., García-España, E. Eds.; Wiley-VCH: New York, 1997. (b) Dietrich, B.; Fyles, T. M.; Lehn, J.-M.; Pease, L. G.; Fyles, D. L. *J. Chem. Soc., Chem. Commun.* **1978**, *21*, 934–936. (c) Schmidtchen, F. P. *Top. Curr. Chem.* **1986**, *132*, 101–133. (d) Dietrich, B. *Pure Appl. Chem.* **1993**, *65* (7), 1457–1464. (e) Sessler, J.-L.; Gale, P. A.; Cho. W.-S. *Anion Receptor Chemistry*; RCS Publishing: London, 2006.

(2) (a) De Silva, A. P.; Gunaratne, H. Q. N.; Gunnlaugsson, T.; Huxley, A. J. M.; McCoy, C. P.; Rademacher, J. T.; Rice, T. E. *Chem. Rev.* **1997**, *97* (5), 1515–1566. (b) De Silva, S. A.; Amorelli, B.; Isidor, D. C.; Loo, K. C.; Crooker, K. E.; Pena, Y. E. *Chem Commun.* **2002**, *13*, 1360–1361.

(3) (a) Prodi, L.; Bolletta, F.; Montalti, M.; Zaccheroni, N. *Eur. J. Inorg. Chem.* **1999**, *3*, 455–460. (b) Passaniti, P.; Maestri, M.; Ceroni, P.; Bergamini, G.; Vötgle, F.; Fakhrnabavi, H.; Lukin, O. *Photochem. Photobiol. Sci.* **2007**, *6* (4), 471–479. (c) Corradini, R.; Dossena, A.; Galaverna, G.; Marchelli, R.; Panagia, A.; Sartor, G. *J. Org. Chem.* **1997**, *62* (18), 6283–6289. (d) Pina, F.; Lima, J. C.; Lodeiro, C.; de Melo, J. S.; Díaz, P.; Albelda, M. T.; García-España, E. *J. Phys. Chem.* **2002**, *106* (35), 8207–8212. (e) Melo, J. S.; Pina, J.; Pina, F.; Lodeiro, C.; Parola, A. J.; Albelda, M. T.; Clares, M. P.; García-España, E. *Phys. Chem.* **2003**, *107* (51), 11307–11318. (f) Bazzicalupi, C.; Bencini, A.; Berni, E.; Bianchi, A.; Giorgi, C.; Fusi, V.; Valtancoli, B.; Lodeiro, C.; Roque, A.; Pina, F. *Inorg. Chem.* **2001**, *40* (24), 6172–6179.

(4) (a) Valeur, B.; Leray, I. *Coord. Chem. Rev.* **2000**, *205*, 3–40. (b) de Silva, A. P.; Fox, D. B.; Huxley, A. J. M.; Moody, T. S. *Coord. Chem. Rev.* **2000**, *205*, 41–57. (c) Prodi, L.; Bolletta, F.; Montalti, M.; Zaccheroni, N. *Coord. Chem. Rev.* **2000**, *205*, 59–83. (d) Fabbrizzi, L.; Licchelli, L. M.; Rabaioli, G.; Taglietti, A. *Coord. Chem. Rev.* **2000**, *205*, 85–108. (e) Parker, D. *Coord. Chem. Rev.* **2000**, *205*, 109–130. (f) Beer, P. D.; Cadman, J. *Coord. Chem. Rev.* **2000**, *205*, 131–155. (g) Robertson, A.; Shinkai, S. *Coord. Chem. Rev.* **2000**, *205*, 157–199. (h) Keefe, M. H.; Benkstein, K. D.; Hupp, J. T. *Coord. Chem. Rev.* **2000**, *205*, 201–228. (i) Pina, F.; Parola, A. J. *Coord. Chem. Rev.* **1999**, *185* (186), 149–165.

(5) (a) Czarnik, A. W. *Acc. Chem. Res.* **1994**, *27* (10), 302–308. (b) Czarnik, A. W. *Fluorescent Chemosensors for Ion and Molecule Recognition*; American Chemical Society: Washington, DC, 1992. (c) Fabbrizzi, L.; Poggi, A. *Chem. Soc. Rev.* **1995**, *24* (3), 197–202.

(6) (a) Bencini, A.; Bernardo, M. A.; Bianchi, A.; Garcia-España, E.; Giorgi, C.; Luís, S.; Pina,F.; Valtancoli, B. In *Advances in Supramolecular Chemistry*; Gokel, G. Ed.; Cerberus Press: Miami, FL, 2002; Vol. *8*, pp 79−130. (b) Parola, A. J.; Lima, J. C.; Lodeiro, C.; Pina, F. In *Fluorescence of Supermolecules, Polymers, and Nanosystems*; Berberan-Santos, M. N. Ed.; Springer-Verlag: Berlin, 2008; Vol. *4*, pp 117−149.

(7) Albelda, M. T.; Aguilar, J.; Alves, S.; Aucejo, R.; Díaz, P.; Lodeiro, C.; Lima, J. C.; García-España, E.; Pina, F.; Soriano, C. *Helv. Chim. Acta* **2003**, *86* (9), 3118–3135.

(8) (a) Ojida, A.; Nonaka, H.; Miyahara, Y.; Tamaru, S.-I.; Sada, K.; Hamachi, I. *Angew. Chem., Int. Ed.* **2006**, *45*, 5518–5521. (b) Anai, T.; Nakata, E.; Koshi, Y.; Ojida, A.; Hamachi, I. *J. Am. Chem. Soc.* **2007**, *129*, 6232–6239.

(9) Aucejo, R.; Alarcon, J.; García-España, E.; Llinares, J. M.; Marchin, K. L.; Soriano, C.; Lodeiro, C.; Bernardo, M. A.; Pina, F.; Pina, J.; de Melo, J. S. *Eur. J. Inorg. Chem.* **2005**, *21*, 4301–4308.

(10) Pina, F.; Passaniti, P.; Maestri, M.; Balzani, V.; Vögtle, F.; Gorka, M.; Lee, S.-K.; Heyst, J. van.; Fakhrnabavi, H. *Chem. Phys. Chem.* **2004**, *5*, 473–480.

Scheme 1

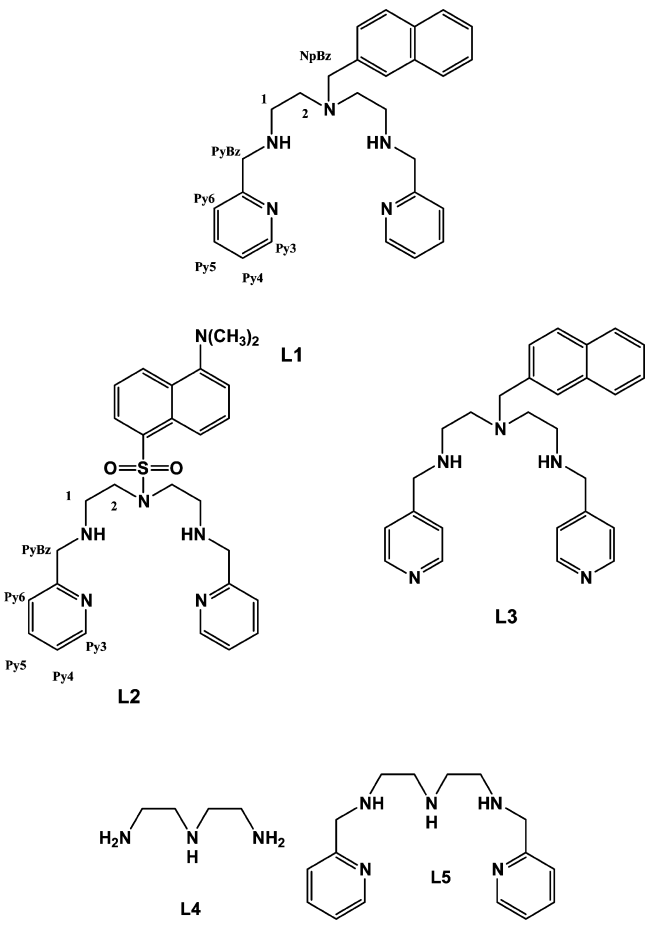

Scheme 2, where the excited naphthalene acceptor, $^1A^*$, forms an intramolecular exciplex, $(A^{\delta-}D^{\delta+})^*$, through a reversible charge transfer from the tertiary amine donor, D.[11]

$$\frac{\varphi_{Exc}}{\varphi_N} = \frac{k'_f}{k_f}\frac{k_1}{k_{-1}+k_{Exc}} \quad (1)$$

The constants k_f and k'_f are the radiative rate constants of naphthalene and exciplex, respectively, k_{ic} and k'_{ic} are the internal conversion rate constants, k_1 is the rate constant for exciplex formation, k_{-1} the rate constant for charge recombination, and $k_{Exc} = k'_f + k'_{ic}$ represents the reciprocal of the decay time of the exciplex in the absence of reversibility ($k_{-1} = 0$).

The plot of $\ln(\phi_{Exc}/\phi_N)$ *versus* the reciprocal of the absolute temperature yields a bell shaped curve with two distinct regimes: the high temperature limit (HTL) where $k_{-1} \gg k_{Exc}$ and $\phi_{Exc}/\phi_N = (k'_f/k_f)(k_1/k_{-1})$ and the low temperature limit (LTL) where $k_{-1} \ll k_{Exc}$ and $\phi_{Exc}/\phi_N = (k'_f/k_f)(k_1/k_{Exc})$. This plot is represented for Zn**L1**$^{2+}$ in the inset of Figure 1C. As in our temperature range, we obtain a straight line with negative slope, it can be inferred that the system is in the LTL regime, and it is possible to extract the activation energy for the exciplex formation, $E_1 = 9.7$ kJ mol^{-1}.

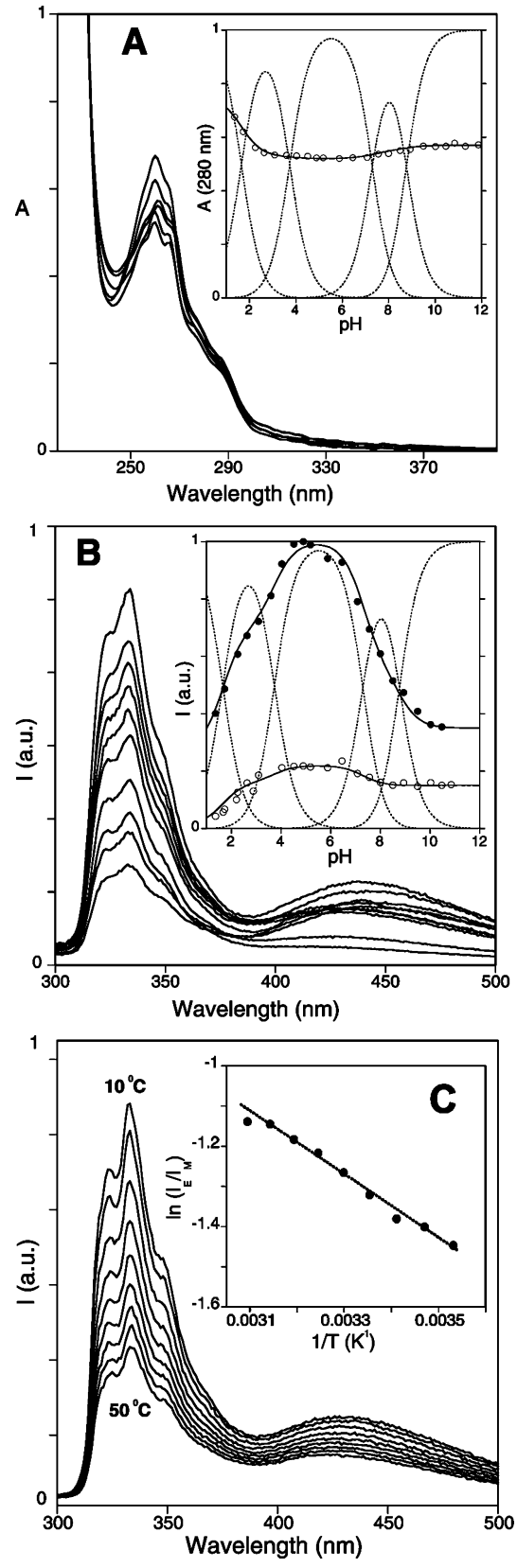

Figure 1. (A) Absorption titration spectra of **L1**, 5.0×10^{-5} M, [NaCl] = 0.15 M; inset: mole fraction distribution together with the titration curves from absorption. (B) Emission titration spectra of **L1** $\lambda_{exc} = 260$ nm; inset: mole fraction distribution together with the titration curves from emission $\lambda_{em} = 335$ nm (●) and $\lambda_{em} = 440$ nm (○). (C) Fluorescence emission of **L1**, at pH = 6.1, as a function of the temperature; inset: $-\ln(I_{Exc}/I_N)$ *vs* $1/T$ plot.

(11) (a) Birks, J. B. *Photophysics of Aromatic Molecules*; Wiley: London, 1970. (b) Bencini, A.; Berni, E.; Bianchi, A.; Fornasari, P.; Giorgi, C.; Lima, J. C.; Lodeiro, L.; Melo, M. J.; de Melo, J. S. A.; Bianchi, A.; Parola, J.; Pina, F.; Pina, J.; Valtancoli, B. *Dalton Trans.* **2004**, *14*, 2180–2187.

Scheme 2

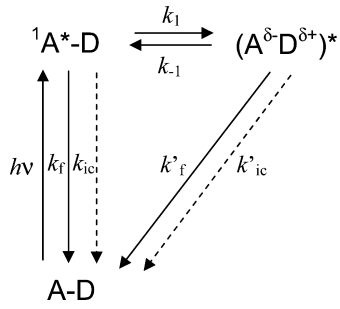

Table 1. Protonation Constants of **L1** Determined by Potentiometry in 0.15 M NaCl at 298.1 ± 0.1 K

reaction	log K_a
$H^+ + \mathbf{L1} = H\mathbf{L1}^+$	8.77(3)
$H\mathbf{L1}^+ + H^+ = H_2\mathbf{L1}^{2+}$	7.54(3)
$H_2\mathbf{L1}^{2+} + H^+ = H_3\mathbf{L1}^{3+}$	3.74(4)[a]
$H_3\mathbf{L1}^{3+} + H^+ = H_4\mathbf{L1}^{4+}$	1.66(2)[a]

[a] Obtained by fluorimetric titration.

Table 2. Fitting Coefficients Obtained for Absorption and Emission Titration of Compound **L1**[a]

species	**L1**	$H\mathbf{L1}^+$	$H_2\mathbf{L1}^{2+}$	$H_3\mathbf{L1}^{3+}$	$H_4\mathbf{L1}^{4+}$
Em (334 nm)	0.35	0.57	1	0.7	0.27
Em (445 nm)	0.15	0.15	0.22	0.16	0.01
Abs (280 nm)	0.57	0.55	0.52	0.53	0.75

[a] Fitting curves shown in Figure 1.

The fluorescence pH titration (inset of Figure 1B) followed either at 335 nm or at 440 nm shows the bell-shaped pattern of the compounds exhibiting a fluorescent pH window.[2,9] At both ends of the curve the quenching is due to a photoinduced electron transfer (PET): from the π-π^* excited-state of the naphthalene to the protonated pyridine at low pH values and from the nonprotonated amines to the π-π^* excited-state of the naphthalene, at higher pH values.[6]

The absorption and the fluorescence emission titration curves were fitted as a linear combination of the mole fraction distribution of the several pH dependent species of compound **L1**; they were calculated with the constants obtained by potentiometry (see Table 1), and the respective fitting coefficients are reported in Table 2.

The fluorimetric titration curve (inset Figure 1B) shows a decrease in fluorescence upon formation of $H_3\mathbf{L1}^{3+}$ and $H_4\mathbf{L1}^{4+}$ in the acidic region. This quenching of the emission suggests that in these species the pyridine rings are being protonated leading to pyridinium moieties that are well-known to quench the naphthalene excited state.[9] Inspection of the absorption fitting coefficients also confirms that for the species $H_4\mathbf{L}^{4+}$ the pyridine moieties are protonated as evidenced by the larger coefficient of the absorption in this species (Table 2), as well as by the shape of the variations (inset of Figure 1A) which are identical to those observed in free pyridine upon protonation. The fact that the absorption coefficient of $H_3\mathbf{L1}^{3+}$ practically does not increase with respect to $H_2\mathbf{L1}^{2+}$ further indicates that the third proton attaches to the central tertiary nitrogen; then, the protons at the terminal secondary nitrogens should be to some extent shared by the pyridine nitrogens which would explain also the decrease in fluorescence. The fourth proton will then be fully attached to the pyridine nitrogens. To get further information about the average protonation sequence in the ground state, we have performed a ^{1}H and ^{13}C NMR study to establish the protonation sequence of **L1**.

It is known that the proton chemical shifts most affected upon protonation of an amino group are those of the ^{1}H nuclei attached to the carbon atoms placed in α-position with respect to it.[12] Therefore, a comparison of the variations with pH of the ^{1}H chemical shifts with the distribution of the protonated species calculated from the macroscopic basicity constants may identify the predominant protonation sequence of a given polyamine. In the case of **L1** this analysis is particularly useful because of the simplicity of its ^{1}H NMR spectrum, Figure 2. At pH 11.4, the ^{1}H NMR spectrum of **L1** consists, in the aliphatic region, of two overlapped triplet signals at about 2.6 ppm corresponding to protons **1** and **2** of the ethylenic chains and of two overlapped singlet signals at 3.63 and 3.64 ppm for the benzylic protons labeled as **NpBz** and **PyBz** (for the labeling, see Scheme 1).

When the pH is decreased to 9.1, where the protonation process has just started, all signals shift downfield appearing now as the triplet signals of **2** and **1** at 2.78 and 2.81 ppm, respectively, the singlet signal of **NpBz** at 3.72 ppm, and that for **PyBz** at 3.79 ppm. The first protonation of the ligand (spectrum at pD = 7.9) yields a further downfield shift of all the aliphatic signals and, in particular, those of **PyBz** ($\Delta\delta$ = 0.21 ppm) and of **1** ($\Delta\delta$ = 0.22 ppm). The shift observed for the other two signals **NpBz** ($\Delta\delta$ = 0.06 ppm)) and **2** ($\Delta\delta$ = 0.11 ppm) being less pronounced. In the aromatic region the doublet signal of protons **Py3** moves slightly downfield from 8.33 to 8.37 ppm. The second protonation (^{1}H NMR at pD = 6.4) produces additional significant downfield changes in the signals of **PyBz** and in the triplet signals of protons **1** ($\Delta\delta$ = 0.18 ppm for both). Again, slight shifts are observed in the chemical shift of **2** and **NpBz** ($\Delta\delta$ = 0.09 ppm). In the same sense, a slight downfield shift is also experienced by the aromatic protons **Py3** ($\Delta\delta$ = 0.05 ppm). These observations support that the first two protonations occur mainly on the secondary nitrogens of the polyamine chain although these protons can be somewhat shared by the central and the pyridine nitrogens (see Scheme 3).

Then, the spectra neither in the aliphatic region nor in the aromatic region show further changes until pD ≅ 3.0 is reached in correspondence with the third protonation of **L1** (see Figure 2, spectrum at pD = 6.4 and pD = 3.9). At these pH values there are important downfield shifts for the triplet signal labeled as **2** ($\Delta\delta$ = 0.28 ppm) and of the singlet signal of **NpBz** ($\Delta\delta$ = 0.32 ppm) both in α-position with respect to the tertiary nitrogen of the polyamine chain. The signals of **1** ($\Delta\delta$ = 0.09 ppm) and of **PyBz** ($\Delta\delta$ = 0.15 ppm) also bear downfield shifts although they are more reduced. The aromatic signal **Py3** shifts downfield 0.13 ppm at this pH. Therefore, these data support that the third protonation

(12) (a) Frassinetti, C.; Alderighi, L.; Gans, P.; Sabatini, A.; Vacca, A.; Ghelli., S. *Anal. Bioanal. Chem.* **2003**, *376*, 1041–1052. (b) Sarnesky, J. E.; Surprenant, H. L.; Molen, F. K.; Reilley., C. N. *Anal. Chem.* **1975**, *47*, 2116–2124.

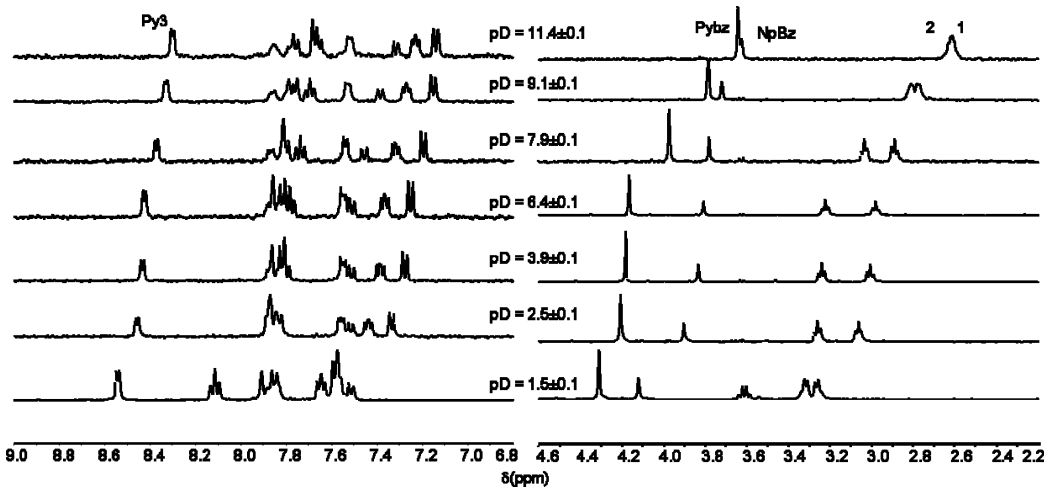

Figure 2. ^{1}H NMR of **L1** in D_2O at several pD values.

Scheme 3. Average Protonation Order of L1 As Derived from ^{1}H NMR, Spectrofluorimetric, and Fluorimetric Data

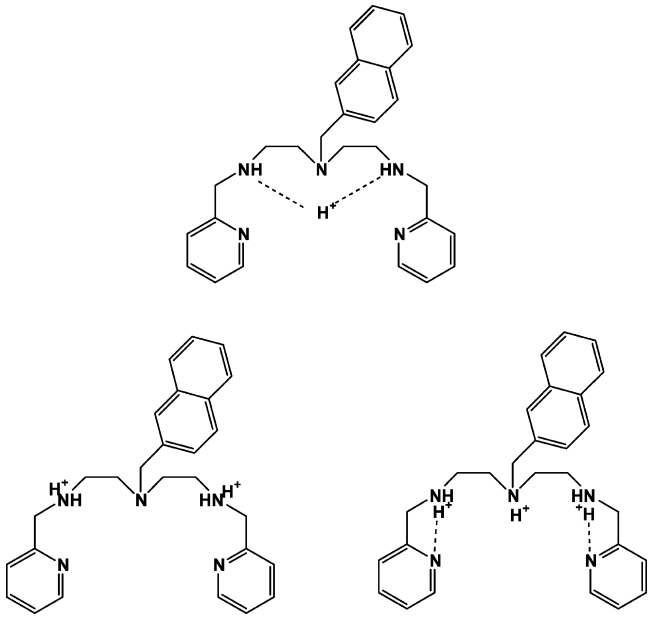

involves the tertiary nitrogen at the middle of the chain. Nevertheless, hydrogen bond formation between the protonated secondary amino groups and the pyridine nitrogens should be favored at this stage as it has been observed in other systems containing 2-pycolyl substituents[13] and is also suggested by the spectral data discussed above.

Looking at the protonation constants (Table 1) it is worth noting that for this compound, and unlike **L3**, the number of protonation constants found indicates that not all the protonable groups of **L1** undergo protonation under the pH range of study. This can be attributed to the internal position of the pyridine nitrogens of **L1** that, upon protonation, will increase the electrostatic repulsion and render the fifth protonation more difficult than in the case of **L3**. Intramolecular hydrogen bonding between the pyridine nitrogens and the adjacent amino groups in **L1** can also contribute to the observed protonation behavior.

Dansyl Sensing Unit. In a previous paper it was reported that for the present receptor,[14] and in contrast to the naphthalene signaling unit, the emission from the dansyl unit occurs in the basic region. This behavior could be convenient for sensing anions because these species are generally deprotonated in the basic region, and in addition, the dansyl emission takes place in the visible region. However, at these basic pH values, the receptor does not possess positive charges to take advantage from the receptor-anion electrostatic attraction, and as a consequence, a different strategy should be used to bring positive charges to the receptor (see below).

Table 3. Stability Constants for the Formation of Zn^{2+} Complexes of **L1** Determined in 0.15 M NaCl at 298.1 ± 0.1 K

species	log *K*
$Zn^{2+} + \mathbf{L1} = Zn\mathbf{L1}^{2+}$	13.01(2)
$Zn\mathbf{L1}^{2+} + H^+ = ZnH\mathbf{L1}^{3+}$	3.65(3)
$Zn\mathbf{L1}^{2+} + H_2O = Zn\mathbf{L1}(OH)^+ + H^+$	−10.76(3)

Similarly to **L1**, the lack of a fully protonated species was also observed for compound **L2**, whose absorption and fluorescence emission titration curves were reported recently.[14] As in the case of **L1**, the two first protonations occur in the polyamine chain, but the third one takes place in the dansyl unit. There is neither from the potentiometry data nor from the fluorescence data any experimental evidence for the protonation of the pyridine units. Nevertheless, they are expected to occur at more acidic values than in the case of **L1**.

Zn^{2+} Complexes of L1 and L2. The potentiometric studies reveal the formation of a monoprotonated and nonprotonated mononuclear species ($ZnH\mathbf{L1}^{3+}$ and $Zn\mathbf{L1}^{2+}$) and one monohydroxylated species ($Zn\mathbf{L1}(OH)^+$) (Table 3). Although it has not yet been possible to obtain suitable crystals for X-ray diffraction, the analysis of the stability constant values and their comparison with related systems, along with the spectroscopic data, can offer hints with respect to the structures in solution.

The stability constant for the $Zn\mathbf{L1}^{2+}$ is higher than the

(13) see for instance (a) Chmielewski, M.; Jurczak, J. *Chem. Eur. J.* **2005**, *11*, 6080–6094. (b) Hossain, M. A.; Kang, S. O.; Powell, D.; Bowman-James, K. *Inorg. Chem.* **2003**, *42*, 1397–1399.

(14) Parola, A. J.; Lima, J. C.; Pina, F.; Pina, J.; Seixas de Melo, J.; Soriano, C.; Garcia-España, E.; Aucejo, R.; Alarcon, J. *Inorg. Chim. Acta* **2007**, *360* (3), 1200–1208.

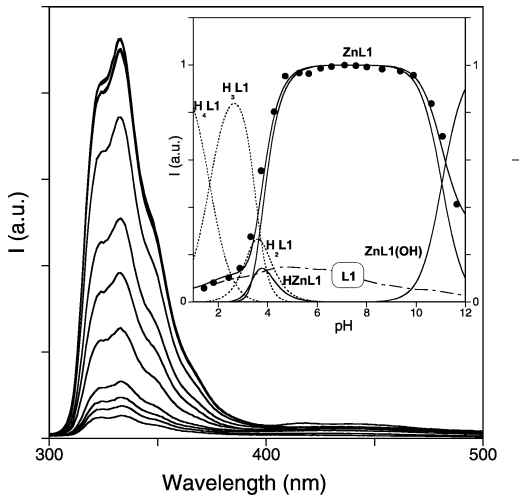

Figure 3. Emission spectra of the complex Zn**L1**$^{2+}$ as a function of pH (λ_{exc} = 260 nm, [Zn**L1**$^{2+}$] = 5.0 × 10^{-5} M, [NaCl] = 0.15 M). Inset: fluorescence emission titration curve of the complex Zn**L1**$^{2+}$, λ_{em} = 335 nm (●), superimposed on the respective mole fraction distribution of species. Traced line: relative fluorescence emission titration of the free ligand.

values found for related systems in which the metal ion is bound by three and four nitrogens. For instance, the stability constant for the formation of the Zn^{2+} complex of **L3** with the pyridine nitrogens at the 4-position pointing outward from the polyamine binding site, in which just the three nitrogens of the polyamine are involved in coordination, is 4.72 logarithmic units,[9] and the Zn**L4**$^{2+}$ complex, with no attached pyridine rings to 1,4,7-triazaheptane (*dien*, **L4** in Scheme 1) is log K = 8.8.[15] The stability constant for the complex Zn**L2**$^{2+}$, in which the two secondary amino groups and the two pyridine nitrogens are coordinated to the Zn^{2+}, is log K = 8.38.[14] Martell et al. obtained for a related polyamine, in which *dien* was functionalized with 2-pycolyl groups (**L5** in Scheme 1), a value of 13.71 logarithmic units for the formation of the pentacoordinated Zn**L5**$^{2+}$ complex.[16] All these data support a likely number of coordinated nitrogen atoms of five with the two secondary nitrogens, the tertiary nitrogen at the middle of the chain, and the two pyridine nitrogens involved in the coordination, although not all them with the same strength as shown by the existence of a monoprotonated ZnH**L1**$^{3+}$ species. The high pK_a obtained (pK_a = 10.76, Table 3) and thereby the low tendency to hydrolyze the Zn**L1**$^{2+}$ species also suggests a pentacoordination of the metal. As discussed in the next paragraph, the fluorescence studies also support this assumption.

The fluorescence emission spectra of compound **L1** in the presence of equimolar amounts of Zn^{2+} and the respective mole fraction distribution of species with pH are reported in Figure 3. The emission titration curves were fitted, like in the case of the free ligand, as a linear combination of the mole fraction distribution of the several pH dependent species present in solution, and the respective obtained coefficients are reported in Table 4.

In the acidic region, the emission is due to the free ligand while in the 5 < pH < 10 region the titration curve is dominated by the intense fluorescence emission of the Zn**L1**$^{2+}$ complex. Some interesting aspects of this system should be emphasized, in particular the comparison between the behavior of the Zn^{2+} complexes of **L1** and the behavior of the parent compound **L3**. In the case of the complex Zn**L3**$^{2+}$, the plateau is very small, and the domain of this species is a sharp curve with maximum peak around pH = 8.0.[9] In contrast, the titration curve of complex Zn**L1**$^{2+}$ exhibits an extended plateau from 5 to 10. This different behavior can be explained by the participation of the pyridine units in the binding. In compound **L3**, these units present the nitrogens in position 4, far from the polyamine chain, while in **L1** the nitrogens are located in position 2, participating in the coordination. The complex is much stronger and as a consequence Zn**L1**$^{2+}$ is the dominant species in a wider pH range.

The Zn^{2+} complex with **L2** was reported previously.[14] As above-mentioned, the lower constant for the formation found for the Zn**L2**$^{2+}$ species (log K = 8.38) reflects the non-involvement of the sulfonamide group in the binding. In this line, the pK_a value obtained for the Zn**L2**$^{2+}$ (pK_a = 9.5) species is lower than that of Zn**L1**$^{2+}$ because it might involve an already coordinated water molecule.

Here, we have performed the additional characterization by ^{1}H NMR. The spectra of **L2** recorded in D_2O at pD = 7.5 (see Figure 4) consists, in the aliphatic region, of one singlet signal at 2.81 ppm that can be assigned to the methyl protons of the dansyl group, two triplets at 2.96 and 3.58 ppm attributable to the methylene groups labeled as **2** and **1** (see Scheme 1) of the ethylenic chain, and another singlet signal 3.86 ppm that corresponds to the methylene benzylic group labeled as **PyBz** (Figure 4A, for the labeling see Scheme 1). In the aromatic region at this pD value one can observe two triplets at 7.33 (**Py5**) and 7.75 ppm (**Py4**) and two doublet signals at 7.16 (**Py6**) and 8.40 ppm (**Py3**) for the protons of the pyridine ring. Apart from these, other four doublets at 7.33 ppm, overlapped with a triplet of the pyridine ring, 8.15, 8.21, and 8.46 ppm and two triplets centered at 7.60 and 7.66 ppm for the protons of the dansyl unit are observed (see Figure 4B). Addition of an equimolar amount of Zn^{2+} produces important changes in the spectra. While the signals of the aliphatic protons **PyBz**, **1**, and **2** shift downfield (**PyBz** appears now at 4.28 ppm, $\Delta\delta$ = 0.42 ppm) and broaden considerably, almost disappearing within the baseline of the spectra, the singlet signal of the methyl groups moves only slightly downfield and does not change its width. Interestingly, in the aromatic region, all the signals of the pyridine protons experience significant downfield shifts, and additionally, those signals of protons **Py3** and **Py4** closer to the aromatic ring broaden considerably (see Figure 4B). The shifts observed in the dansyl protons are much less noticeable. These data support the involvement of the pyridine nitrogens in the coordination of the metal ion and exclude the participation of the $N(CH_3)_2$ moiety of the dansyl unit in the binding. A likely coordination mode is depicted for Zn**L1**$^{2+}$ and Zn**L2**$^{2+}$ in Figure 5, although additional

(15) Martell, A. E.; Smith, R. M.; Moteikaitis, R. M. *NIST Critical Stability Constants Database*; Texas A&M. University: College Station, TX, 1993.

(16) Harris, W. R.; Murase, I.; Timmons, J. H.; Martell, A. E. *Inorg. Chem.* **1978**, *17*, 889–894.

Table 4. Fitting Coefficients Obtained for the Emission Titration of Complex Zn**L1**$^{2+}$ (λ_{exc} = 260 nm, λ_{em} = 335 nm)[a]

species	H_4**L1**$^{4+}$	H_3**L1**$^{3+}$	H_2**L1**$^{2+}$	H**L1**$^{+}$	**L1**	ZnH**L1**$^{3+}$	Zn**L1**$^{2+}$	Zn**L1**(OH)$^{+}$
Zn**L1**$^{2+}$ complexes	0.045[b]	0.12[b]	0.17[b]			0.3	1	0.3

[a] Fitting curve shown in Figure 3. [b] The coefficients relative to the free ligand contribution were divided by 5.6 since the normalization here was made from the emission of the Zn**L1**$^{2+}$ species, which is 5.6-fold more emissive than the H_2**L1**$^{2+}$ species.

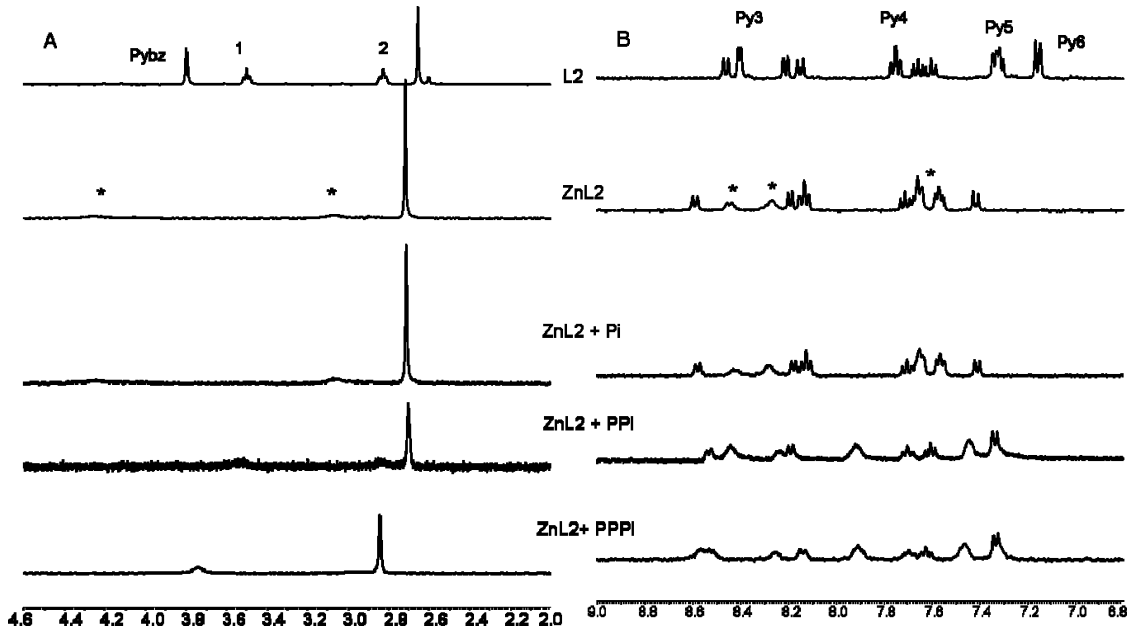

Figure 4. ^{1}H NMR spectra of **L2**, Zn**L2**$^{2+}$, and phosphate (Pi), diphosphate (PPi), and triphosphate (PPPi) in D_2O at pD = 7.5 ± 0.1 at room temperature.

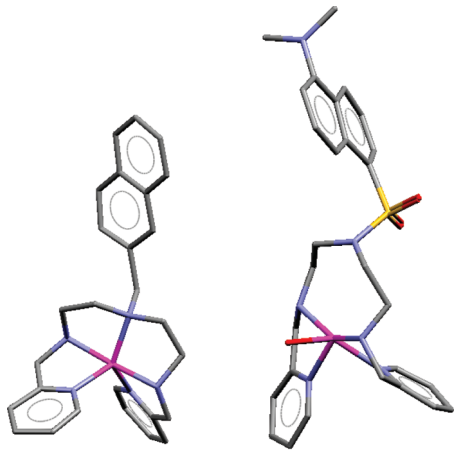

Zn**L1**$^{2+}$ Zn**L2**$^{2+}$

Figure 5. Proposed coordination modes for Zn**L1**$^{2+}$ and Zn**L2**$^{2+}$. Additional water molecules could complete hexacoordination.

molecules of solvent could complete a hexacoordination for the metal.

During our fluorescence measurements of Zn**L2**$^{2+}$ it was verified that, while for small excitation slits the emission is reproducible, when the intensity of the excitation light is high a new, more intense, and blue-shifted emission band is formed, see Figure 6. A similar spectroscopic feature was previously described in the framework of the outstanding work of Kimura and co-workers on model compounds for Zn^{2+} enzymes as a result of formation of strong bonds between aromatic sulfonamides and Zn^{2+}.[17] In particular, a fluorophore possessing a *cyclen* receptor unit and a dansyl signaling moiety exhibits such a behavior at pH = 7.3. The

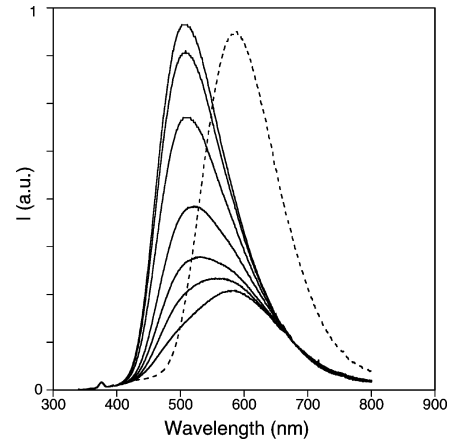

Figure 6. Irradiation of the compound Zn**L2**$^{2+}$ at 333 nm, pH = 7.3: 0, 5, 10, 15, 20, 25, 30 min, full lines; free ligand (traced line) 5.0×10^{-5} M, [NaCl] = 0.15 M.

dansyl group is deprotonated and the nitrogen binds strongly to the metal, leading to a blue-shifted new fluorescence emission band whose intensity increases about 5-fold. In the present compound, the nitrogen of sulfonamide is tertiary but there is still an electron pair available to coordinate the metal. Although this is not an usual situation in the ground state, there are some reports on tertiary sulfonamide binding to metal ions.[18] Taking into account that the excited dansyl unit is reached from a charge transfer from the dimethy-

(17) (a) Koike, T.; Watanabe, T.; Aoki, S.; Kimura, E.; Shiro, M. *J. Am. Chem. Soc.* **1996**, *118*, 12696–12703. (b) Aoki, S.; Sakurama, K.; Matsuo, N.; Yamada, Y.; Takasawa, R.; Tanuma, S. I.; Shiro, M.; Takeda, K.; Kimura, E. *Chem.—Eur. J.* **2006**, *12* (35), 9066–9080. (c) Kimura, E.; Koike, T. *Chem. Commun.* **1998**, (15), 1495–1500.

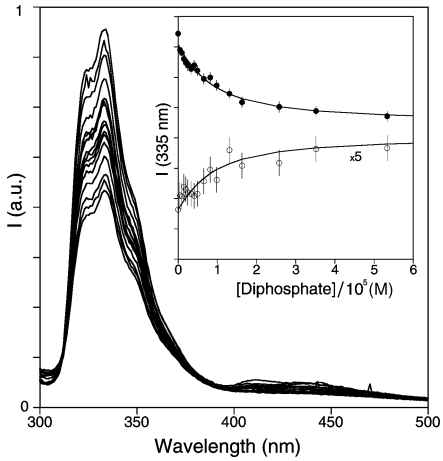

Figure 7. Emission spectra of the complex Zn**L1**$^{2+}$ at pH = 8 as a function of diphosphate ion concentration (λ_{exc} = 265 nm, [Zn**L1**]$^{2+}$ = 5.0 × 10^{-6} M, [NaCl] = 0.15 M). Inset: Fluorescence intensity at 335 nm vs. diphosphate concentration (●); the line represents the fitting of the experimental points assuming a 1:1 stoichiometry and log K = 5.2.

lamino-substituted aromatic moiety to the sulfonamide, the excess of charge in this nitrogen in the excited-state might be the driving force to remove water from the intimate coordination sphere of the metal giving rise to a nitrogen−metal bond. The bond Zn^{2+}−dansylsulfonamide would lead to a fluorescence pattern similar to that found by Kimura and coworkers.[17]

Sensing Anions with Zn^{2+} Complexes. Anion sensing usually takes advantage of hydrogen bonding and electrostatic interactions. The search for a positive charge in the receptor can be achieved by amine protonation, but the use of metal complexes such as those of Zn^{2+} is an alternative, as described in this section.

The fluorescence emission of free **L1** is only slightly affected by the addition of anions. Experiments were carried out at pH = 6 (maximum emission of **L1**), and a very small increase of its emission (∼7%) is observed. In contrast, solutions containing the Zn**L1**$^{2+}$ complex at pH = 8, in the middle of the emission plateau presented by this species (see Figure 3), were used to detect the presence of several anions. The changes in fluorescence observed upon titration of Zn**L1**$^{2+}$ with diphosphate are shown in Figure 7. Addition of diphosphate to the solution containing Zn**L1**$^{2+}$ leads to about 1/3 decrease in emission intensity, and a value of log K = 5.2 can be obtained by fitting the data on the basis of a 1:1 stoichiometry. The quenching effect can be explained by the interaction of the metal with the anion leading to a decrease of the protecting effect of the metal and to PET from the aliphatic amine to the excited naphthalene.

Similarly, significant decreases in the fluorescence intensity were observed for citrate, cyanurate, triphosphate, and iodide ions. The changes in fluorescence intensity with anion concentration yield acceptable fits with 1:1 stoichiometry (see Supporting Information), and the respective association constants are collected in Table 5. Phosphate, fluoride and D,L-isocitrate gave rise to a decrease in fluorescence of less than 10%, which renders the determination of the association constants for these anions very difficult.

Table 5. Association Constants of Several Anions with Zn**L1**$^{2+}$ (1:1) Obtained from the Fitting of the Fluorimetric Titrations ([Zn**L1**]$^{2+}$ = 5 × 10^{-6} M, pH = 8.0, 25 °C, [NaCl] = 0.15 M)

anion	log K^a
triphosphate	5.8
diphosphate	5.2
phosphate[b]	
iodide	5.5
fluoride[b]	
citrate	5.5
D,L-isocitrate[b]	
cyanurate	5.5

[a] Estimated error: 4%. [b] Phosphate, fluoride, and D,L-isocitrate show changes in fluorescence below 10%, and an accurate determination of the constant is not possible in these cases.

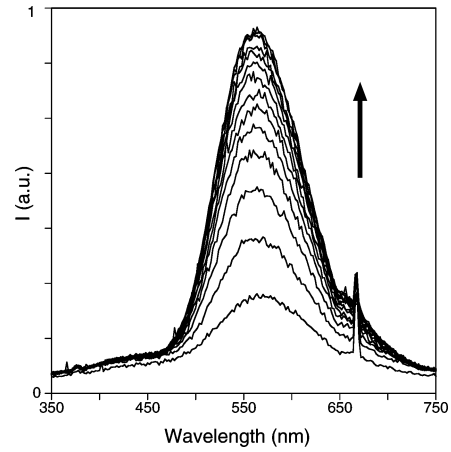

Figure 8. Fluorescence emission of the compound Zn**L2**$^{2+}$ in the presence of increasing concentrations of triphosphate ion at pH = 7.5, in [NaCl] = 0.15 M, λ_{exc} = 333 nm.

These high values for log K compare relatively well with those determined by Anslyn et al. for the interaction of Cu^{2+} complexes with several anions in water using spectrophotometry.[19] Interesting enough is the fact that all association constants are quite high, independently of the negative charge of the anion, showing that the association is not driven exclusively by electrostatic interactions. A similar situation was also observed by Anslyn.[19]

The fluorescence changes occurring to Zn**L2**$^{2+}$ upon addition of some triphosphate are reported in Figure 8. Differently from the sensor bearing the naphthalene, the dansyl emission that was partially quenched by complexation with the metal is restored by addition of anions. Considering that the quenching by the metal occurs by a photoinduced electron transfer mechanism from the excited dansyl unit to the electron-deficient Zn^{2+}-pyridine moiety, the presence of negative charges in the vicinity of the cavity is expected to decrease the probability of the electron transfer process, rendering the "pyridinium" less electron-deficient. The system exhibits good sensitivity, and its selectivity is able to discriminate between three sets of anions: (i) those like triphosphate that tend to restore the fluorescence emission

(18) (a) Calligaris, M.; Carugo, O.; Crippa, G.; Desantis, G.; Dicasa, M.; Fabbrizzi, L.; Poggi, A.; Seghi, B. *Inorg. Chem.* **1990**, *29* (16), 2964–2970. (b) Klingele, M. H.; Moubaraki, B.; Murray, K. S.; Brooker, S. *Chem.—Eur. J.* **2005**, *11* (23), 6962–6973. (c) Sun, C. H.; Chow, T. J.; Liu, L. K. *Organometallics* **1990**, *9* (3), 560–565.

(19) Tobey, S. L.; Jones, B. D.; Anslyn, E. V. *J. Am. Chem. Soc.* **2003**, *125* (14), 4026–4027.

Table 6. Association Constants of Several Anions with Zn**L2**$^{2+}$ Obtained from the Fitting of the Fluorimetric Titrations ([Zn**L2**]$^{2+}$ = 5 × 10^{-5} M, pH = 7.5, 25 °C, [NaCl] = 0.15 M)

anion	log K^a
triphosphate (class A)	4.9
diphosphate (class A)	4.1
phosphate (class B)	
iodide (class B)	
fluoride (class B)	
cyanurate (class B)	
citrate (class C)	2.7
D,L-isocitrate (class C)	2.1

[a] Estimated error: 4%.

by CHEF, Figure 8, class A; (ii) those like cyanurate that hardly affect the fluorescence emission of the complex, class B; (iii) others like citrate and D,L-isocitrate that restore the fluorescence emission of Zn**L2**$^{2+}$ but less efficiently than phosphates, class C. The classification of the studied anions is given in Table 6. This selectivity is very significant in comparison with other systems reported in the literature.[20]

To further characterize the mixed Zn^{2+}-**L2**-anion complexes, ^{1}H and ^{31}P NMR, as well as electrospray mass spectrometry studies, were carried out at pD about 7.5. We have selected as representative cases the systems Zn^{2+}-**L2**-phosphate, Zn^{2+}-**L2**-diphosphate, Zn^{2+}-**L2**-tripolyphosphate, Zn^{2+}-**L2**-citrate, and Zn^{2+}-**L2**-D,L-isocitrate, which are collected in Figures 4, 9, and 10. As can be seen in Figure 9, addition of phosphate does not produce significant changes in the ^{31}P NMR spectra. The shift observed in the ^{31}P NMR signal ($\Delta\delta$ = 0.62 ppm, Figure 9) could be attributed to a weak electrostatic interaction between the charged metal complex and the anion. The electrospray mass spectra do not show any peak attributable to the formation of mixed species. However, addition of either diphosphate or triphosphate produces significant changes both in the ^{1}H and ^{31}P NMR spectra. In the presence of diphosphate, the 2-fold symmetry is preserved but the aliphatic signals of protons **1**, **2**, and **PyBz** move significantly upfield (Figure 4A). The same type of changes is observed in the aromatic region with the pyridine protons signals becoming even broader than for the binary system (Figure 4B). In the ^{31}P spectrum there is an observed downfield shift from −7.93 to −5.79 ppm when free diphosphate coordinates to Zn**L2**$^{2+}$ at this pH ($\Delta\delta$ = 2.15 ppm), Figure 9. Similar changes are observed in the ^{1}H NMR spectra for the system Zn^{2+}-**L2**-triphosphate (see Figure 4). In the ^{31}P NMR spectra, downfield shifts of 2.51 ppm and of 4.38 ppm are observed for the terminal and central phosphorus nuclei (Figure 9), as well as a broadening of the signal, particularly for the triplet signal of the central phosphorus nucleus. The ESI spectra recorded on the same NMR samples shows in the positive mode peaks at m/z = 522.1 which corresponds to the free ligand with deuterium substitution of the two protons, likely those of the NH groups, and at m/z = 584.1, 683.5, and 839.4 due to Zn**L2**$^{2+}$ − H$^+$, Zn**L2**(ClO$_4$)$^+$, and Zn**L2**(PPP)$^{3-}$ + 4H$^+$, respectively.

For the anions derived from the tricarboxylic acids citrate and D,L-isocitrate, the ^{1}H NMR and ESI spectra recorded at the same pH values of the fluorimetric titrations confirm also the formation of mixed complexes. Addition of citrate yields upfield shifts of the signals of protons **PyBz**, **1**, and **2** of the ligand (Figure 10). The observed shifts are, although more moderate, similar to those of the polyphosphate anion systems (for instance, for **PyBz** $\Delta\delta$ = 0.15 ppm). In contrast with case of the polyphosphate anions, here the singlet signal of the methyl groups of dansyl moves slightly upfield $\Delta\delta$ about 0.06 ppm). The AB spin system signal (J = 15.8 Hz) of the citrate equivalent CH_2 groups does not change its spin pattern upon interaction with Zn**L2**$^{2+}$ although it also shifts upfield ($\Delta\delta$ = 0.09 ppm). In the aromatic region, a generalized upfield shift is observed for all the signals.

In the case of the system Zn**L2**$^{2+}$-D,L-isocitrate, the ^{1}H NMR, apart from downfield shifts, reveals a very interesting alteration in the spin system of the CH_2 group of the carboxylate which, upon interaction with the complex, changes from a classical ABX system (J_{AB} = 15.4 Hz, J_{BX} = J_{AX} = 7.6 Hz) to a broad doublet (J = 7.1 Hz) which supports an equivalence of the protons in the NMR time scale (see Figure 10). The spin-couplings of the other two proton signals remain unmodified. This may suggest that the binding of the isocitrate moiety occurs through the carboxylate closer to the CH_2 group (see Figure 11).

The ESI spectra in the negative mode are very clear and show, for both systems, peaks at m/z = 774.0 ppm which corresponds to [Zn**L2**(cit)]$^-$ or to [Zn**L2**(isocit)]$^-$ species with two protons substituted by deuterium.

Conclusions

Through this work it was shown that sensing anions by means of Zn^{2+} complexes of polyamine based sensors can be achieved if the proper design is carried out. The metal introduces the positive charge needed to bind anions taking benefit from the electrostatic attraction. On the other hand the choice of the sensing unit is also crucial. CHEQ or CHEF can take place according to the type of sensing unit appended to the receptor. In the case of the dansyl sensing unit, the fluorescence appears in the visible region, and the presence of the pyridine unit in the chain is crucial because this moiety is responsible for the partial quenching in the metal complex, which permits the CHEF effect of the anion. While remarkable anion discrimination was found in the case of the system Zn**L2**$^{2+}$−anion, the selectivity found in the case of the Zn**L1**−anion system is still a drawback of the system, and further improvements on this line should be carried out to render these systems appealing for possible applications. In any case, this work emphasizes the relevance of classical metal complexes in anion discrimination through the many possibilities that the coordinative bond offers.

Experimental Section

Synthesis. L1 was synthesized following the general procedure described for **L3** in ref 9. In the last step, 2-pyridinecarbaldehyde (1.00 g, 9.34 mmol) dissolved in 100 mL of EtOH was added to 100 mL of an ethanolic solution of 4-(2-naphthylmethyl)-1,4,7-triazaheptane (1.13 g, 4.67 mmol). The mixture was stirred at room temperature for 4 h. Then, $NaBH_4$ (0.44 g, 11.50 mmol) was added

(20) Schneider, H.-J.; Yatsimirsky, A. K. *Chem. Soc. Rev.* **2008**, (2), 263–277.

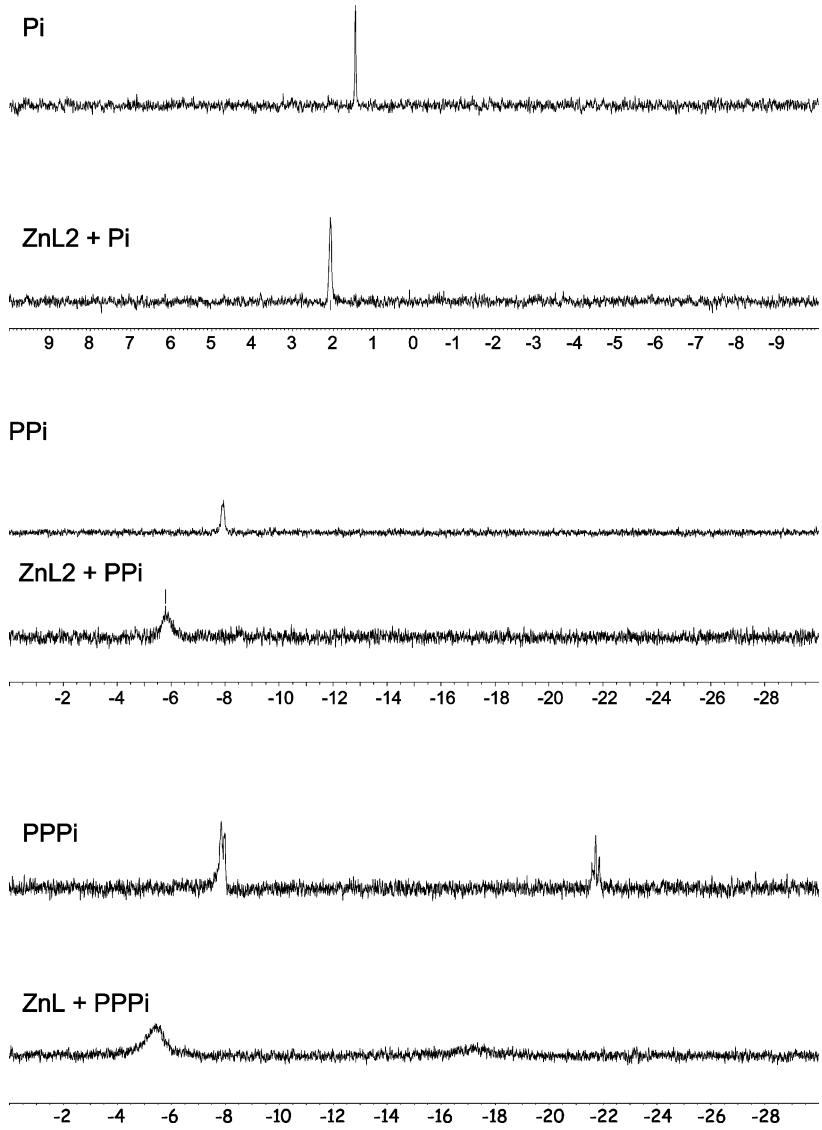

Figure 9. ^{31}P NMR of Zn**L2**$^{2+}$ in D_2O with phosphate (Pi), diphosphate (PPi), and triphosphate (PPPi) at pD = 7.5.

in portions. The reaction was kept under stirring for another 2 h at room temperature, and the solvent was vacuum evaporated to dryness. The residue was treated with 50 mL of water and extracted with CH_2Cl_2 (3 × 40 mL). The organic phase was dried with anhydrous sodium sulfate, and the solvent evaporated to dryness. The amine was purified by column chromatography using $CHCl_3$−MeOH 95:5 v/v as eluent. The resulting oil was dissolved in EtOH, and **L3** was precipitated as its pentahydrochloride salt with aqueous HCl (1.47 g., 52%). ^{1}H NMR (D_2O): δ = 3.35 (m, 8 H), 4.22 (s, 2 H), 4.38 (s, 4 H), 7.46 (m, 3 H), 7.78 (m, 7 H), 7.85 (s, 1 H), 8.25 (m, 2 H), 7.54 (d, *J(H−H)* = 5.2 Hz, 2 H). ^{13}C NMR (D_2O): δ = 43.9, 48.3, 50.5, 59.4, 127.4, 127.5, 127.8, 128.2, 128.4, 129.5, 130.1, 130.4, 133.0, 130.4, 133.0, 133.3, 144.3, 146.1, 146.2. Anal. Calcd. for $C_{27}H_{40}Cl_5N_5$ (607.9): C, 53.4; H, 6.0; N, 11.5. Found: C, 53.4; H, 5.9; N, 11.4%.

Emf Measurements. The potentiometric titrations were carried out at 298.1 ± 0.1 K with 0.15 M NaCl as the supporting electrolyte. The experimental procedure (burette, potentiometer, cell, stirrer, microcomputer, etc.) has been fully described elsewhere.[21] The acquisition of the emf data was performed with the computer program PASAT.[22] The reference electrode was a Ag/AgCl electrode in saturated KCl solution. The glass electrode was calibrated as a hydrogen-ion concentration probe by titration of previously standardized amounts of HCl with CO_2-free NaOH solutions, and the equivalent point determined by Gran's method,[23] which gives the standard potential, $E^{\circ\prime}$, and the ionic product of the water (pK_w = 13.7381).

The computer program HYPERQUAD[24] was used to calculate the protonation and stability constants. The pH range investigated was 2.5−11.0, and the concentration of the ions and the ligand ranged from 1×10^{-3} to 5×10^{-3} M. The different titration curves for each system (at least two) were treated either as a single set or as separate curves without significant variations in the values of the stability constants. Finally, the sets of data were merged together and treated simultaneously to give the final stability constants.

(21) Garcia-España, E.; Ballester, M. J.; Lloret, F.; Moratal, J. M.; Faus, J.; Bianchi, A. *J. Chem. Soc., Dalton Trans.* **1988**, (2), 101–104.

(22) Fontanelli, M.; Micheloni, M. *Proceedings of the I Spanish-Italian Congress on Thermodynamics of the Metal Complexes*, Diputación de Castellón, Castellón, Spain, 1990. Program for the automatic control of microburette and the acquisition of the electromotive force readings.

(23) (a) Gran, G. *Analyst (London)* **1952**, *77* (920), 661–671. (b) Rossotti, F. J.; Rossotti, H. *J. Chem. Educ.* **1965**, *42* (7), 375–378.

(24) Sabatini, A.; Vacca, A.; Gans, P. *Coord. Chem. Rev.* **1992**, *120*, 389–405.

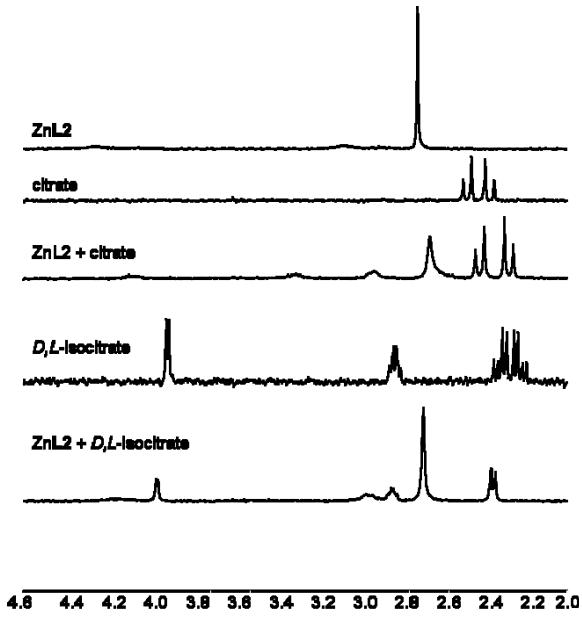

Figure 10. ^{1}H NMR spectra of Zn**L2**$^{2+}$ and citrate, D,L-isocitrate in D_2O at pD = 7.5 ± 0.1.

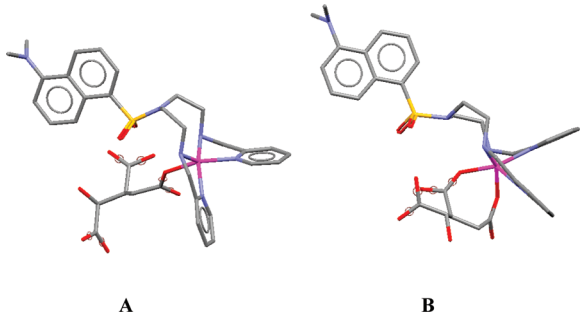

Figure 11. Possible binding modes of D,L-isocitrate to Zn**L2**$^{2+}$. (A) monodentate, (B) bidentate.

Spectrophotometric and Spectrofluorimetric Measurements. Absorption spectra were recorded on a Shimadzu UV-2501PC spectrophotometer and fluorescence emission spectra on a Horiba-Jobin-Yvon SPEX Fluorolog 3.22 spectrofluorimeter at 25 °C. In the case of fluorimetric titrations with **L2**, narrow slits had to be used: excitation slits of 0.5 nm, emission slits of 3 nm; in the case of **L1**, the corresponding values were both 3 nm. HCl and NaOH were used to adjust the pH values, which were measured on a MeterLab 240 pH meter. All measurements were made in 0.15 M NaCl and in a pH range 7.8 < pH < 8.1, where the emission of the Zn**L1**$^{2+}$ species reaches a plateau. Because the association constants are quite high, low concentrations of ligand **L1** (5×10^{-6}M) had to be used. To the ligand solution at pH = 8 was added an equimolar amount of a concentrated solution of $Zn(NO_3)_2$ to form the 1:1 Zn/**L1** complex. The pH was checked and eventually adjusted to 8. The titrations were carried out by addition of aliquots of 0.0010 M solutions of the anions prepared at pH = 8. After each addition, the pH was measured and adjusted to 8 whenever necessary. An identical procedure was used in the case of **L2**.

The absorption and fluorimetric titration data, normalized to the more absorbing or emissive species, were fitted using weighted sums of the mole fractions of the species (obtained by potentiometry). The weight factors were the molar absorptivities and the product of molar absorptivity and fluorescence quantum yield.[25]

The association constants of the complexes with the anions were obtained from the fit of the fluorimetric titration data with the general equation reported in ref 26.

NMR Measurements. The ^{1}H and ^{31}P NMR spectra were recorded on Bruker Advance 400 operating at 399.91 MHz for ^{1}H and at 161.88 MHz for ^{31}P. For the ^{13}C NMR spectra, dioxane was used as a reference standard (δ = 67.4 ppm), and for the ^{1}H spectra, the solvent signal. Adjustments to the desired pH were made using drops of DCl or NaOD solutions. The pD was calculated from the measured pH values using the correlation, pH = pD − 0.4.[27]

ESI Mass Spectroscopy. ESI-MS spectra were recorded with an Esquire 300 (Bruker) by electrospray positive mode (ES^+) or negative modes (ES^-).

Molecular Modeling. Molecular models in Figures 5 and 11 were produced with HYPERCHEM version 7.5. (Hypercube (2005) for illustration purposes only.[28]

Acknowledgment. L.R. acknowledges Post-Doc Grant SFRH/BPD/26882/2006 from FCT-MCTES (Portugal). Financial support from CTQ2006-15672-CO5-01 (Spain) and CTQ2006-15672-CO5-04, Generalitat Valenciana (GV06/258) and Fundação para a Ciência e Tecnologia is gratefully acknowledged. J. M. Ll. thanks MCYT of Spain for a Ramón y Cajal Contract.

Supporting Information Available: Spectrofluorimetric titrations of the complex Zn**L1**$^{2+}$ at pH = 8 as a function of anion concentration (λ_{exc} = 265 nm, [Zn**L1**$^{2+}$] = 5.0×10^{-6}M, [NaCl] = 0.15M) and the respective fittings of the emission at 335 nm, assuming a 1:1 stoichiometry; Figure S1, triphosphate and phosphate; Figure S2, iodide and fluoride; Figure S3, citrate, isocitrate, and cyanurate (PDF). This material is available free of charge via the Internet at http://pubs.acs.org.

IC7023956

(25) Bernardo, M. A.; Parola, A. J.; Pina, F.; Garcia-España, E.; Marcelino, V.; Luis, S. V.; Miravet, J. F. *J. Chem. Soc., Dalton Trans.* **1995**, 993.
(26) Čudić, P.; Žinić, M.; Tomišić, V.; Simeon, V.; Vigneron, J.-P.; Lehn, J.-M. *J. Chem. Soc., Chem. Commun.* **1995**, 1073–1075.
(27) Covington, A. K.; Paabo, M.; Robinson, R. A.; Bates., R. G. *Anal. Chem.* **1968**, *40*, 700–710.
(28) *HYPERCHEM* Version 7.5; Hypercube Inv.: 1115 NW 4th St., Gainsville, FL.